Theta Band-Power Shapes Amyloid-Driven Longitudinal EEG Changes in Elderly Subjective Memory Complainers At-Risk for Alzheimer's Disease

Giuseppe Spinelli[a,b,*], Hovagim Bakardjian[b], Denis Schwartz[f], Marie-Claude Potier[a], Marie-Odile Habert[c,d,e], Marcel Levy[b], Bruno Dubois[a,b] and Nathalie George[a] on behalf of the INSIGHT-preAD Study Group

[a]*Institut du Cerveau - Paris Brain Institute - ICM, Inserm, CNRS, APHP, Sorbonne Université, Hôpital de la Pitié Salpêtrière, Centre MEG-EEG, CENIR, Paris, France*
[b]*Institute of Memory and Alzheimer's Disease (IM2A), Department of Neurology, AP-HP, Hôpital de la Pitié-Salpêtrière, Paris, France*
[c]*CNRS, INSERM, Laboratoire d'Imagerie Biomédicale, Sorbonne Université, Paris, France*
[d]*AP-HP, Hôpital de la Pitié-Salpêtrière, Médecine Nucléaire, Paris, France*
[e]*Centre d'Acquisition et Traitement des Images (CATI), Paris, France*
[f]*CERMEP-Imagerie du Vivant, Lyon, France*

Abstract.
Background: Alzheimer's disease (AD) includes progressive symptoms spread along a continuum of preclinical and clinical stages. Although numerous studies uncovered the neuro-cognitive changes of AD, very little is known on the natural history of brain lesions and modifications of brain networks in elderly cognitively-healthy memory complainers at risk of AD for carrying pathophysiological biomarkers (amyloidopathy and tauopathy).
Objective: We analyzed resting-state electroencephalography (EEG) of 318 cognitively-healthy subjective memory complainers from the INSIGHT-preAD cohort at the time of their first visit (M0) and two-years later (M24).
Methods: Using ^{18}F-florbetapir PET-scanner, subjects were stratified between amyloid negative (A–; $n = 230$) and positive (A+; $n = 88$) groups. Differences between A+ and A– were estimated at source-level in each band-power of the EEG spectrum.
Results: At M0, we found an increase of theta power in the mid-frontal cortex in A+ compared to A–. No significant association was found between mid-frontal theta and the individuals' cognitive performance. At M24, theta power increased in A+ relative to A– individuals in the posterior cingulate cortex and the pre-cuneus. Alpha band revealed a peculiar decremental trend in posterior brain regions in the A+ relative to the A– group only at M24. Theta power increase over the mid-frontal and mid-posterior cortices suggests an hypoactivation of the default-mode network in the A+ individuals and a non-linear longitudinal progression at M24.

*Correspondence to: Giuseppe Spinell, Paris Brain Institute – ICM, 47 Bd. de l'Hôpital, 75013 Paris, France. E-mail: giuseppespinelli88@gmail.com.

Conclusion: We provide the first source-level longitudinal evidence on the impact of brain amyloidosis on the EEG dynamics of a large-scale, monocentric cohort of elderly individuals at-risk for AD.

INTRODUCTION

Alzheimer's disease (AD) is the most prevalent neurodegenerative disease and the most common form of dementia (approximately 60–80% of dementia cases; Alzheimer's Association, 2015). AD primarily affects elderly individuals (∼65 years; Alzheimer's Association, 2015) and includes cognitive symptoms and biological signs spread along a continuum of pre-clinical (pre-AD) and clinical stages. Symptoms mainly include impairments in cognitive functions and loss of memory, while biological signs consist in potentially irreversible neuro-physio-pathological alterations including senile plaques, neurofibrillary tangles, and inflammatory changes [1, 2]. Despite many scientific efforts, the large heterogeneity of AD phenotype and the non-linear progression of both signs and symptoms render clinical and pharmacological trials mostly ineffective. Indeed, no efficient drug exist to slow the progression of AD (success rate for approval is ∼0.4% [3]). Cognitive therapies limit to link life-long cognitive stimulations and trainings to an extended tolerance to the onset of AD symptoms (i.e., the so-called "cognitive reserve" hypothesis; [4, 5]) or other forms of cognitive impairment [6–8], but no decisive solution has emerged yet. Therefore, AD has become a huge public health problem, counting a broad increasingly number of people living with dementia worldwide (∼46.8 million individuals, predicted to double every 20 years).

From a pathophysiological point of view, the most credited theory on the AD pathogenesis is the amyloid cascade hypothesis [9, 10] which posits that brain amyloid-β (Aβ) accumulation is the key event which triggers neuronal damage, synaptic function impairments and ultimate widespread neurodegeneration. Crucially, all these events appear many years before the onset of clinical symptoms [11, 12] and are thought to cause a so-called disconnection syndrome [13]: brain functional and structural connections become progressively and irreversibly disrupted. Moreover, Aβ load is supposed to behave as an accelerator of other consequent biochemical events [14] together with genetics [15] and sex

[16–19], thus resulting in additive risks of developing AD. Therefore, two phases are now considered in the AD continuum: a preclinical phase of more than 15 years and a clinical one which encompasses a prodromal (predementia) and a dementia stage [20]. Given the lack of efficacy of disease-modifier therapies in patients with dementia, scientific interest has grown on individuals at-risk for AD, that is, showing the earliest signs of neuropathological events (i.e., amyloid or tau pathology) in the absence of AD-related cognitive symptoms [20]. Characterizing the neurophysiological patterns of cognitively normal individuals with high Aβ load has thus become one of the most crucial challenges in clinical neuroscience, with the hope of better understanding the functional correlates of risk factors to AD and ultimately being able to predict the progression of AD.

In this vein, electroencephalography (EEG) has been used for many years to acquire a direct, non-invasive view of human brain activity in condition of physiological and pathological aging (i.e., AD or other dementias). Indeed, EEG allows an extremely precise discrimination of the temporal hierarchy governing distributed brain networks at different frequencies, i.e., 1–4 Hz (delta), 4–8 Hz (theta), 8–13 Hz (alpha), 13–30 Hz (beta), and >30 Hz (gamma), thus allowing to investigate the information that these canonical frequencies may convey on various mental and physiological states. In this regard, physiological aging is characterized by both a marked "slowing" of the background EEG (see [21], for a review) and a decreased power of the occipital alpha-band which, in turn, is typically accompanied by an increase of slower frequencies, i.e., delta and theta [22–24]. Despite this, healthy seniors often show plastic compensatory brain mechanisms which contribute to relatively long-term functional maintenance and absence of any symptoms. When symptoms become sufficiently evident, albeit not severe enough to exceed standard critical criteria for AD, mild cognitive impairment (MCI) emerges. A meta-analysis conducted on 56 non-demented seniors, 106 MCI, and 108 AD patients showed an intermediate magnitude of alpha power in parieto-occipital brain areas in MCI with respect to the other two groups [25]. Such a

decrease of alpha power has been linked to a dysregulation of the thalamo-cortical and cortico-cortical brain networks governed by the cholinergic brainstem pathway, which is thought to be responsible of the transmission of sensori-motor information and the retrieval of semantic information [26]. Besides alpha, lower frequencies of the EEG power spectrum have also been associated to different neural peculiarities of MCI. More specifically, while delta power has been inversely associated to cortical atrophy [24], both theta band-power and theta interhemispheric coherence were found to be predictive of the decline from MCI to AD [27]. Taken together, these findings corroborate the idea that MCI can be considered as a transitive stage between physiological aging and AD, not only from a clinical [28], but also from an electrophysiological point of view. For what concerns AD, EEG studies convincingly showed an increase widespread delta and theta power and a decreased posterior alpha power in comparison with both normal seniors and MCI [25, 29–32]. Interestingly, alpha decrease is generally associated to impaired cognitive function as indexed by neuropsychological tests and batteries, such as the Mini-Mental-State Examination (MMSE) [33]. Characterization of posterior alpha power has also allowed discrimination among different phenotypes of dementias [34, 35]. Decreased of posterior alpha power or of the so-called individual-alpha peak (i.e., the frequency associated to the strongest EEG power within the standard alpha range) differentiates mid-AD from early-AD [36], cerebrovascular dementia, frontotemporal dementia, and early-stages of AD [31, 37]. Moreover, classification of theta power has been used to explain subtle working memory changes in AD [38], as well as to differentiate AD dementia from Lewy body dementia [39]. Relevant for the present work are studies showing the association between additional biological parameters and cortical EEG markers in AD. Specifically, increased genetic risk of AD—as indexed by presence of *Apolipoprotein E* (*APOE*) ε4 genotype—is thought to affect spontaneous electrical activity [40], in both theta and beta bands [41], as well as global EEG connectivity [42–44]. In this respect, although connectivity measures have become fine-grain markers to better characterize changes of brain network dynamics, findings in AD are not homogeneous and there is still no consensus on which connectivity analysis (e.g., local connectivity, global connectivity, network assortativity, or graph analysis) or which measure of connectivity (e.g., real/imaginary coherence, phase-locking value,

network-node, or entropy) may reliably reflect brain changes along the AD continuum [45–55]. Moreover, recent evidence by Frisoni et al. [56] suggested that the current amyloid-driven model of AD fits particularly autosomal dominant AD but is less applicable to sporadic AD, thus rendering the conceptualization of the biology of AD and related quantification with neuroimaging methods more complex.

In view of all this evidence, investigating the EEG changes associated with amyloidosis (that is, Aβ burden) in elderly cognitively normal individuals with subjective memory complaint, who may be considered at-risk for developing AD, has become tremendously relevant for the scope of AD research. To the best of our knowledge, only a few EEG studies have been reported in this domain. Target cohorts typically include individuals with increased risk to convert to AD, such as elderly subjective cognitive/memory complainers with or without positive biomarker status for AD, e.g., cortical amyloidosis [20, 57]. In particular, Babiloni et al. [58] revealed an increase of frontal lower frequency bands at source level in a group of 53 subjective memory complainers as compared to 79 healthy seniors and 143 MCI (both amnesic and not-amnesic). Prichep et al. [59] reported that mid-frontal theta band power was able to predict the conversion from non-pathological aging to MCI in a group with subjective cognitive decline. This finding was replicated by Gouw et al. [60] who showed that theta power increase on mid-frontal scalp locations characterized the conversion to MCI in a sub-group of non-demented seniors with an amyloid positive biomarker status. Noteworthy, the scarce control of 1) any underlying neuropathology (i.e., amyloid status or genetic profile), 2) the inter-subject variability due to scarce homogenization of the studied population, and 3) the exclusion of neurological comorbidities and mixed-type symptoms, and the relatively small sample sizes, limit the generalization of these findings.

The ongoing longitudinal INSIGHT-preAD cohort study (INveStIGation of AlzHeimer's PredicTors in subjective memory complainers) was setup to address these issues [61]. First resting-state EEG investigations on this cohort at the baseline period, that is, at the time of the first visit (i.e., M0), revealed contradictory results. While Teipel et al. [62] revealed no association between amyloid burden and scalp-level regional EEG connectivity, Gaubert et al. [63] mainly showed an increased connectivity within a fronto-central scalp network as a function of the amyloid status and the degree of neurodegeneration.

In the present work, we capitalize on these findings to further evaluate the longitudinal impact of cortical amyloid load on the resting-state EEG pattern of elderly subjective memory complainers of the INSIGHT-preAD cohort. Source-level EEG analyses guarantees a more fine-grained exploration of the neural dynamics of this population, while longitudinal approach provides with a more robust test of any long-term effect as well as a characterization of the brain network changes. In addition, we tested for genetic influence (presence of the *APOE ε4* allele), for the confounding effects of sex and age, and for any association between EEG features and individuals' cognitive performance.

METHODS

Sample

Participants were selected from the INSIGHT-preAD study [61], a French monocentric cohort including longitudinal data of 318 seniors without objective cognitive impairment (185 females; mean-age: 76.1 years, range: 70–85 years) recruited from the Institute for Memory and Alzheimer's Disease (IM2A) at the Pitié-Salpetriere Hospital of Paris. All of them had complained about memory issues for more than 6 months before the recruitment. To be included in the cohort, participants should have normal cognitive abilities (MMSE score ≥27; Clinical Dementia Rating score = 0) and no objective memory deficits (Total recall score ≥41 at the Free and Cued Selective Reminding Test). Written informed consent was collected at the time of the first visit (i.e., baseline or M0). The study conformed to the 1975 Declaration of Helsinki and was approved by the local ethics review board. To study longitudinally the neurophysiological profile of the cohort, data referring to the first (M0:318 participants) and to the 2nd year visit (M24:279 participants) were extracted. Following quality-check and artefact rejection (see below), the data of 272 subjects, matched across the two visits (M0, M24) were included in the analyses (see Table 1 for further details).

Neuropsychological assessment

Patients' cognitive profile was assessed by a comprehensive neuropsychological battery including: the MMSE [33], the Clinical Dementia Rating [64], the Digit Span [65], the Free and Cued Selective

Table 1
Demographic characteristics, global cognitive profile, amyloid status, and *APOE* genotype of the sample

		M0	M24
Participants (female)		*318 (185)*	*279 (172)*
Education (y)		*6.2 ± 2.1*	
Age ± SD		*76.1 ± 3.5*	
MMSE ± SD		*28.7 ± 0.96*	
FAB ± SD		*16.4 ± 1.73*	
FCSRT-TR ± SD		*46.1 ± 1.98*	
Amyloid status	A– │ *APOE ε4+*	*230 │ 25*	*206 │ 24*
	A+│ *APOE ε4+*	*88 │ 33*	*75 │ 29*

SD, standard deviation; MMSE, Mini-Mental State Examination; FAX, Frontal Assessment Battery; FCSRT-TR, Free and Cued Selective Reminding Test-total recall.

Reminding Test (FCSRT), Letter and Category Verbal Fluency test, the Rey Complex Figure Copy [66], the Trail Making Test [67], the Frontal Assessment Battery [68], the Memory Capacity Test [69], and the Digit Symbol Substitution Test [70]. Further details are provided in Table 1.

PET-amyloid scan

A Philips Gemini GXL CR-PET scanner served to measure the amyloid uptake in the brain. Scans were acquired 50 (±5) min after injection of ~370 MBq (range: 333–408 MBq) of ^{18}F-florbetapir. The acquisition consisted in 3×5 min frames, 128×128 acquisition matrix with a $2 \times 2 \times 2$ mm^3 voxel size. Images were reconstructed by means of the LOR-RAMPLA algorithm with 10 iterations and a smooth post-reconstruction filter was applied. Frames were then realigned, averaged and quality-checked by the CATI team (http://cati-neuroimaging.com). Composite cortical regions of interest (ROIs) (left/right-pre-cuneus, posterior-cingulate cortex, and anterior cingulate cortex, parietal, temporal and orbitofrontal cortices) were derived and a reference region (i.e., pons and whole cerebellum) was placed in the individual native PET space. Parametric PET images were created by dividing each voxel to the mean activity of the reference region. Standard amyloid uptake value ratios (SUVr) were extracted by averaging the mean values across all cortical ROIs. Based on a linear conversion of the CAEN method to the INSIGHT cohort [71, 72], individuals with a SUVr >0.79 were classified as amyloid positive (A+) while individuals with a SUVr ≤0.79 were classified as amyloid negative (A–) (see Table 1) [20, 72].

APOE genotype

DNA was extracted from frozen blood samples by applying the 5Prime Archive Pure DNA purification method. Genotypes were determined using Sanger method (see [61] for details). Individuals were then split in groups based on their *APOE* genotype and assigned to sub-samples of carriers (ε4+) or non-carriers (ε4-) of at least one *APOE* ε4 allele (i.e., ε4/ε4 and ε4/ε3) (Table 1).

MRI acquisition

A 3T Siemens Verio MRI scanner (Siemens Medical Solution, Erlangen, Germany) equipped with a 12-channel head coil for signal reception was used for MRI acquisition. For the anatomical study, 3D MPRAGE sequences were acquired (sagittal orientation, 2300 ms, 2.98 ms echo time, 900 ms inversion time, 9° flip angle, 176 slices with a 1 mm thickness, field of view of 256*240 mm, and a bandwidth of 240 Hz/Px) [61].

EEG recording and analysis

Resting-state EEG (rsEEG) was acquired at 250 Hz using a 256-channel whole-head cap (EEG System GES 300, Electrical Geodesic, Inc) and amplified by the EGI NetAmp300. No modification of the signal was applied at recording. The reference electrode was Cz. Electrodes impedance was kept below 50 kΩ. Each rsEEG was acquired in two separate 2-min runs. Each run consisted in two consecutive sequences of 60 s recording in which participants were instructed to keep their eyes closed (EC; 30 s) and opened (EO; 30 s). A low- or high-frequency tone was delivered to indicate the onset of each EC or EO condition, respectively. To minimize blinking, each rsEEG run was preceded by a fixation cross (2 s) presented at the center of a computer-screen against a black background. The NetStation 4.4 software (EGI) was used for signal acquisition, and the E-Prime software (Psychology Software Tools, Inc, PA, USA) allowed the synchronization of marker-events (onset and end of each EC/EO periods) in each recording sequence.

Neural time series were pre-processed using the Fieldtrip toolbox (release: July 2017) [73] in Matlab r2016a (The MathWork, Inc). Each dataset was filtered with a 1–80 Hz band-pass FIR filter (one-pass, zero-phase). Artifact detection was restricted to scalp-electrodes ($n = 173$) and carried out by means of a thresholding procedure, such that three metrics were calculated for each sensor along the whole time-series (i.e., variance, amplitude-range, and minimum voltage value) and then transformed in z-scores based on the mean and the standard deviation of the whole scalp-electrodes set. Sensors with |z-scores|$\geq$2.5 for at least one of the three metrics, were marked as artifactual and excluded from the analysis. On average, 5.4 channels (range: 1–13) were rejected for each participant. The resulting artifact-free channels were used to re-reference the time series to a common-average referencing. A visual inspection of the continuous data was carried out to exclude segments of data exhibiting any residual aberrant activity (mainly due to muscular artifacts). Then, an Independent Component Analysis (ICA) was run to correct blinks/oculomotor artifacts. ICs showing highest correlations with signals recorded from both the peri-orbital and peri-canthal planes were removed from the original signals. On average, 2.3 ICs referring to eye artifacts (range: 1–6) were removed.

Source localization of oscillatory brain activity was carried out by means of the beamformer method [74, 75]. For each subject, EC and EO EEG signals were band-pass filtered (FIR filter; one-pass, zero phase) into 7 frequency bands (delta [2–4 Hz], theta [4–8 Hz], alpha$_1$ [8–10 Hz], alpha$_2$ [10–13 Hz], beta$_1$ [13–20 Hz], beta$_2$ [20–30 Hz], and gamma [30–40 Hz]). For each of these band-pass filtered traces, the data covariance matrix was calculated after merging EO with EC. A common-spatial filter was obtained by means of a Linearly Constrained Minimum Variance (i.e., LCMV [75]) beamformer and multiplied to each EC and EO condition to project the data in the source-space. The forward solution (Boundary Element Method) was obtained from a dipolar model based on a 3-compartments mesh (i.e., brain, skull, scalp) created on each individual's MRI through FreeSurfer processing as implemented in the FieldTrip toolbox. Voxel positions were derived from individual's MRI and normalized to a 5-mm grid covering the entire brain. Alignment between the MRI and the EEG coordinate system was carried out by marking three fiducial points (i.e., nasion, left- and right- pre-auricular) on individual MRIs. Source-level data were then normalized in the MNI space. To match EEG source reconstructed activity to anatomically meaningful brain regions, the source space was segmented into 90 ROIs using Automated Anatomical Labelling (AAL) [76].

Frequency analysis was performed at voxel-level by means of a multi-tapered Fast Fourier Transform

using a Hanning taper. Band-power was computed by taking the squared magnitude of the real and imaginary Fourier spectra. The relative power was obtained by dividing the power in a single band by an estimate of the summed power, i.e., the sum of the power in the 7 bands. These values were ultimately transformed into z-scores (using the mean and the standard deviation across voxels) to enable comparisons between subjects and frequencies. To exclude outliers from each visit, a 95% confidence interval was computed across subjects using the global power over all the frequency bands, such that subjects exhibiting values >95% were discarded from the analysis.

To test statistically the effect of brain amyloidosis on source-level power for each visit a Monte Carlo cluster-based permutation approach was implemented [77], with 5000 iterations. For each frequency band, a permutation distribution of the significance probabilities for independent-samples t-tests between A– and A+ was calculated. The significant threshold of both cluster-alpha and alpha was set at 0.05, and the maximum of the sum of t-values within each cluster was considered as the test statistic [77]. To circumvent the issue of unequal variance and sample-size of the two groups (i.e., A+ and A–), a bootstrap-like procedure was applied to the permutation test, as described in Mewhort et al. [78]. Data from the larger group (i.e., A–) were selected at random to create a sample of equal size as the smaller group (i.e., A+) and then the Monte-Carlo cluster-based permutation test was run on this subset of the data. This procedure was implemented 100 times, each time noting whether and where (in which brain region) the independent-samples t-test rendered any significant cluster (positive and/or negative). The proportion of cases (out of 100) in which a given significant effect replicated was calculated to estimate the reliability of the initial cluster-based test.

A further exploration was carried out on the link between rsEEG activity and the severity of brain amyloidosis. Band-power data were extracted from the significant cluster of voxels and related to SUVr values distributed in 7 evenly spaced cumulative probabilities quantiles in order to have an equal number of cases per probabilities quantile. Then, a between-subjects ANOVA was run using the SUVr as independent variable (7 levels). Bonferroni method was used to correct for multiple comparisons.

The association between subjects' electrophysiological profile and cognitive abilities was assessed

by means of a linear regression model predicting regional specific band-power spectra from individuals' memory performance (as indexed by the FCSRT-TR test).

To further explore the additive contribution of the *APOE* genotype status, a between-subjects ANOVA was run, considering the power values extracted from the significant cluster(s) as the dependent measure, the amyloid status (2 levels: A– and A+) and the *APOE* status (2 levels: $\varepsilon+$ and $\varepsilon-$) as independent variables, and both the sex (dichotomic) and the age (continuous) as covariates.

RESULTS

Cortical dynamics at M0

Electro-cortical markers of brain amyloidosis

The contrast between the neurophysiological profile of A– and A+ subjects revealed significant differences in the theta-band [4–8 Hz] only, at the time of the first visit (i.e., M0; Fig. 1a, b). A+ exhibited an increase of theta-band power in comparison with A– (cluster-statistic: –98.33, $t = 5.01$, $p < 0.02$ [cluster-corrected]; Fig. 1c). According to the AAL atlas coordinates, this effect localized on a bilateral mid-frontal cluster of voxels including the rectus gyrus, the frontal superior and medial orbital cortex and the anterior cingulate cortex. The reliability of the test, i.e., the number of times in which the test resulted in the same identical effect, was 82% (82 cases out of 100). Moreover, the vincentization of amyloid load showed that the theta enhancement was parametrically modulated by the severity of brain amyloidosis ($F_{(6,265)} = 6.3$, $p < 0.001$, $\eta^2 = 0.99$): subjects with a higher accumulation of cortical amyloid (i.e., quantiles 6-7) showed a greater increase of mid-frontal theta-power in comparison of those with a below-threshold amyloid deposition (i.e., quantiles 1–5; $p < 0.01$; Fig. 1d). This pattern was replicated by a linear regression model ($r^2 = 0.08$, $p < 0.001$) considering continuous amyloid values as predictors of mid-frontal theta power (Fig. 1e).

Exploring any additive effect of APOE genotype, sex, and age

The significant main effect of amyloid load on mid-frontal theta power ($F_{(1,271)} = 19,34$, $p < 0.001$) was not affected by the confounding covariates of age ($p = 0.52$) and sex ($p = 0.99$), and, importantly,
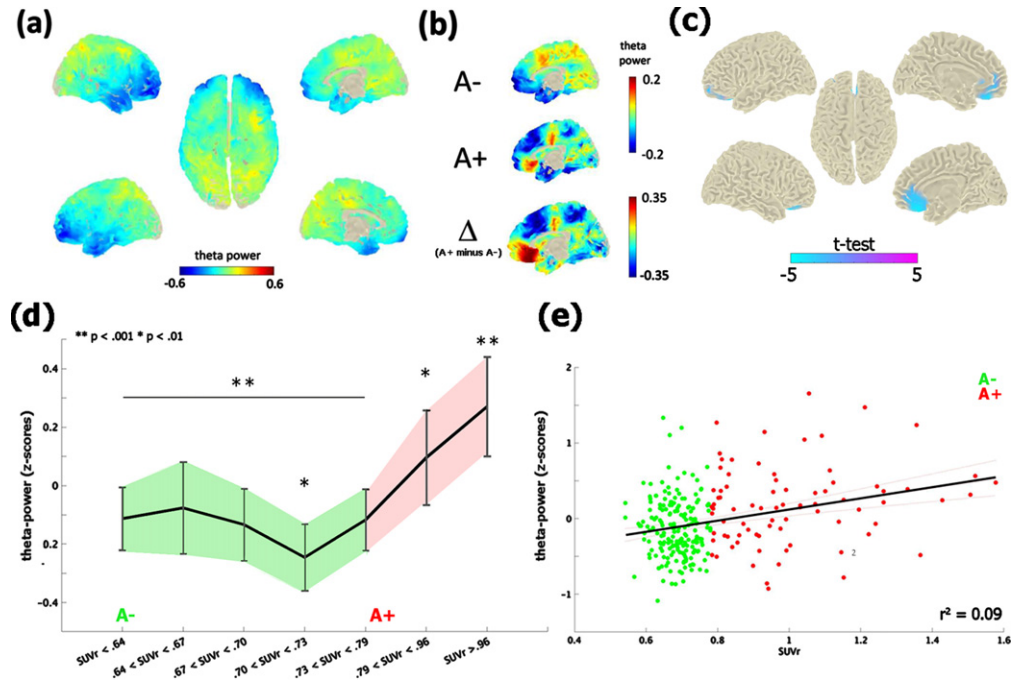
Fig. 1. Theta-band power distribution on the brain surface at the time of the first visit (i.e., M0). Panel (a) depicts the grand-mean across the whole sample. Panel (b) shows the difference between A+ and A−. Values are expressed in z-scores. Panel (c) highlights the contrast between the groups (i.e., A− versus A+) computed through an independent-samples t-test. Significant probabilities are corrected at cluster-level by means of a Monte Carlo permutation approach. Note: negative t-test (in cyan) on the mid-frontal brain regions reflects ampler theta-power for A+ relative to A−. Panel (d) depicts the significant increase of theta-power as a function of amyloid deposition. Continuous values of amyloid are distributed in 7 quantiles, each including averaged theta-power values of ∼38 subjects. In this, individuals with highest amyloid deposition (i.e., quantile 7; A+) shows a higher (**$p < 0.001$) increase of mid-frontal theta-band power with respect to A− (i.e., quantiles 1–5). A moderate effect (*$p < 0.01$) is also shown between the middle (i.e., quantile 4) and medium-high stages of amyloid deposition. Vertical bars indicate 95% confidence interval. The scatterplot in panel (e) shows the linear regression between continuous values of amyloid and mid-frontal theta power.
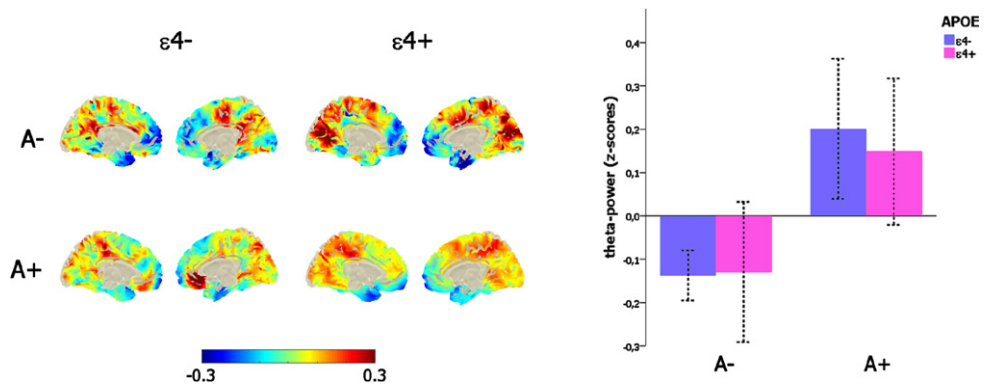

Fig. 2. Link between mid-frontal theta-band power, amyloid deposition, and *APOE* genotype. Left-column depicts the theta-power distribution on the brain surface (left-column) as a function of the amyloid (i.e., A− versus A+) and *APOE* (i.e., ε4− versus ε4+) status. The bar-plot (right-column) represents the variation of mid-frontal theta power as a function of amyloid (i.e., A− versus A+) and *APOE* (i.e., ε4− versus ε4+) status.
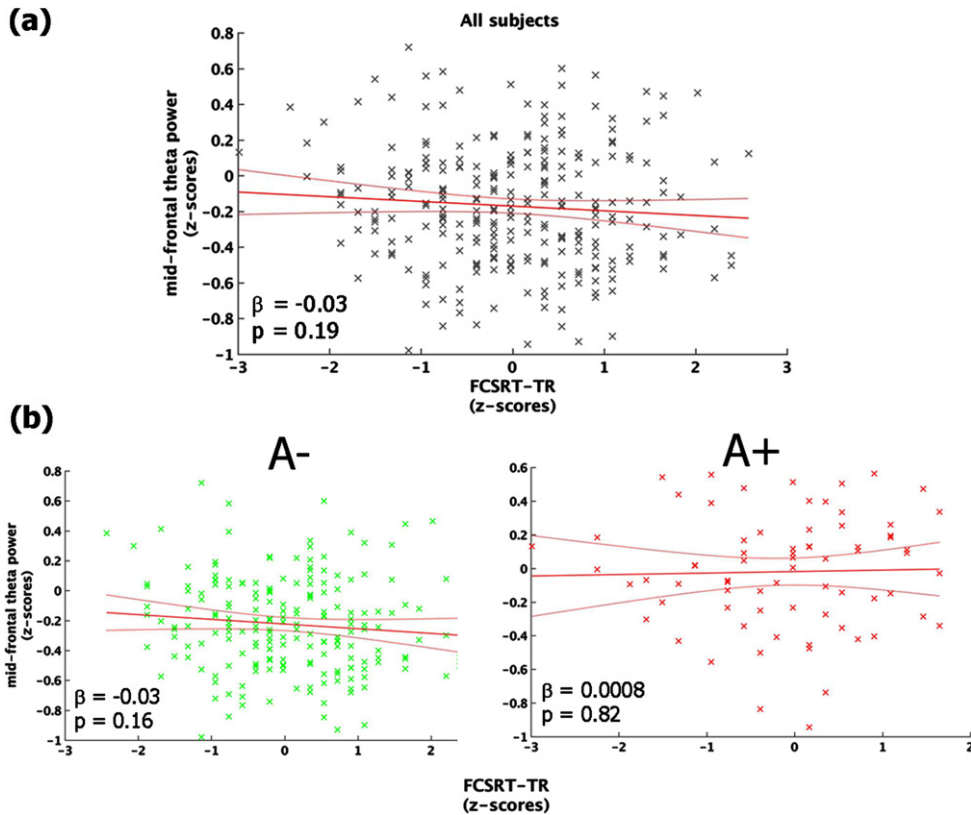
Fig. 3. Link between mid-frontal theta-band power and memory performance (FCSRT-TR). Panel (a) shows the linear regression model carried out on the whole sample. Panel (b) depicts the same model performed on A− (left-column) and A+(right-column), separately. All the plot shows the raw data (black/green/red stars), the fit of the model (red straight-line) with 95% confidence interval (red curved-line), its slope (β-coefficients) and the associated *p*-value.

there was neither any main effect of APOE genotype ($p = 0.75$) nor any interaction between the amyloid (i.e., A− versus A+) and the APOE status ($\varepsilon 4$- versus $\varepsilon 4$+; $p = 0.64$; Fig. 2c).

Linking neurophysiological patterns and cognitive performance

The regression between FCSRT-TR and mid-frontal theta power showed a non-significant inverse trend ($F_{(1,270)} = 1.67$, $p = 0.19$, $r^2 = 0.006$, $r^2_{adjusted} = 0.002$) explained by the fact that individuals with decreased memory performance tended to exhibit higher values of mid-frontal theta power (Fig. 3a). The same analysis conducted in the two groups (i.e., A+ and A−) separately, indicated that the aforementioned trend was mainly accounted for by people with a lower cortical amyloid load (i.e., A−: $F_{(1,198)} = 1.92$, $p = 0.15$; A+: $F_{(1,70)} = 0.19$, $p = 0.67$; Fig. 3b).

Cortical dynamics at M24

We conducted similar analyses at the time of the second-year follow-up (i.e., M24), in all frequency-bands. The only significant effect or trend were found in the theta and alpha bands.

Theta band-power

The previous mid-frontal theta-band power increase shown at M0 by A+ participants was not replicated. However, the analysis showed a significant bilateral increase of theta-band power in a posterior midline brain region including the pre-cuneus, the posterior-cingulate cortex, and the calcarine fissure (cluster-statistic: −100.15, $t = 4.8$, $p < 0.02$ [cluster-corrected]; Fig. 4). The bootstrap-like procedure indicated that this effect was replicated in 44% of cases when considering a random subsample of A− participants of equal size as the A+ group, pointing to a likely greater variability in the A− group.
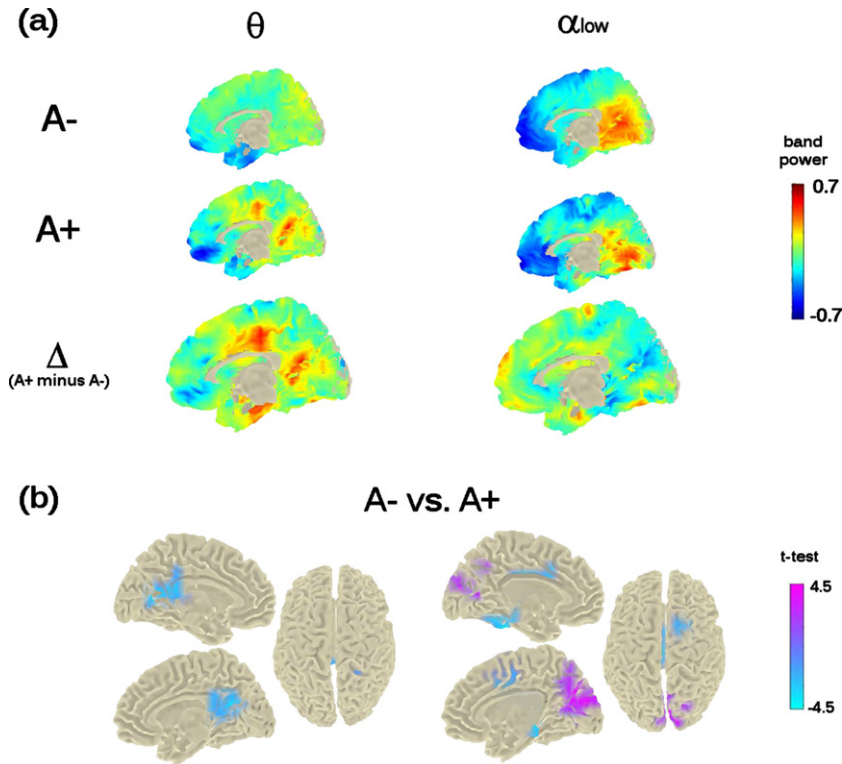
Fig. 4. Theta- and Alpha-low band power distribution on the brain surface at the time of the second visit (i.e., M24). Panel (a) depicts the grand-mean across the whole sample for A– and A+ as well as the difference between A+ and A–. Power-values are expressed in z-scored as for M0. Panel (b) shows the independent-samples *t*-test computed between A– and A+. Negative *t*-test (in cyan) reflects ampler band-power for A+ with respect to A–; positive *t*-test (in magenta) reflects lower band-power for A+ with respect to A–. Importantly, significant probabilities are cluster-corrected for theta-band (left-column) and not at all corrected for alpha-low (right-column).

Alpha band-power

The analysis run on alpha band, considering both low-alpha and high-alpha bands, showed a significant effect only in the $alpha_1$ band (8–10 Hz; $p < 0.05$). Individuals with an increased risk to develop AD (i.e., A+ individuals) showed a decreased power in the cortical region around the parieto-occipital sulcus and the calcarine fissure (Fig. 4), in keeping with previous investigations on MCI and AD. However, this effect did not resist the cluster correction (Fig. 4, top- and bottom-right raw). No significant differences were found for $alpha_2$ (10–13 Hz).

Teasing apart the role of APOE genotype, sex, and age

The significant main effect of amyloid deposition on mid-caudal theta power at M24 ($F_{(1,271)} = 6.8$, $p < 0.05$) was not affected by the confounding covariates of age ($p = 0.12$) and sex ($p = 0.17$). No main effect of APOE genotype ($p = 0.58$) nor any interaction between the amyloid and the APOE status

was found. The regression between mid-caudal theta power and FCSRT-TR showed no significant effect.

DISCUSSION

In this study, we provide the first EEG evidence of the impact of cortical amyloid deposition on the longitudinal resting-state neuro-dynamics of elderly subjective memory complainers from the standardized, large-scale INSIGHT-preAD cohort. We found an increase of theta-band power in the mid-frontal cortex in the group of individuals with a higher (A+) compared to a lower (A–) amyloid deposition at the time of the first visit (M0), regardless of the individual APOE status, sex, and age. No significant association was found between mid-frontal theta power and individuals' cognitive performance. Noteworthy, while the very same effect was not replicated at the second-year follow-up (M24), theta-band power was found to be increased in A+ relative to A– individuals in

the posterior cingulate cortex and the pre-cuneus. Moreover, an ad-hoc analysis computed on the alpha band revealed a trend to a decrease of low-alpha band power in the brain regions surrounding the calcarine cortex and the parieto-occipital sulcus, in the A+ relative to the A– group. However, this latter effect did not resist the multiple comparisons correction.

Theta neurodynamic changes have been frequently reported in previous EEG investigations on the AD continuum. In particular, widespread theta (and delta) band-power increase is one of the most prominent markers of the so-called "EEG slowing" occurring in physiological aging and has been linked to individuals' cognitive and memory decline [21]. Studies on MCI and AD further support this idea. In fact, both theta band-power increase and theta-driven inter-hemispheric coherence are predictive hallmarks of the conversion from MCI to AD [27] and differentiate AD from other dementias [32, 39]. As regards the pre-AD stages, mid-frontal theta power is thought to be linked to the progression from physiological aging to the prodromal (predementia) stage of clinical AD both in the absence [59] and in the presence [60] of cortical amyloid deposition. A recent cross-sectional investigation on the INSIGHT pre-AD cohort also reported a significant sensitivity of mid-line theta scalp connectivity to brain amyloid load [63]. Our data nicely fit with all these findings and bring new insights not only on the cortical sources of theta band, but also on the prominent impact that amyloid load has on these EEG sources. Such a peculiar sensitivity of mid-frontal theta rhythms to brain amyloidosis in healthy subjects at risk for AD may first be viewed in the face of the impact that early amyloid deposition (and its spreading trajectories) has on the temporo-frontal neural networks. Amyloid plaques initially deposit on the temporal neocortex and disrupt the neural circuits connecting this region with the pre-frontal cortex [11]. It has been shown that theta oscillations orchestrate the communication between pre-frontal areas and the hippocampus [79, 80], and govern many hippocampal-prefrontal-driven cognitive functions, such as spatial working memory [81], navigation [82], memory formation [83], and memory integration [84]. Moreover, given that mid-frontal cortex is a key region of the default mode network (DMN) and that theta oscillations are inversely related to the activation of the DMN [85], we suggest that high amyloid load leads to an hypoactivation of the DMN which ultimately manifests as a mid-frontal theta band hyperactivation at the macroscopic scale. DMN functional alteration is

reported in a large amount of brain imaging studies on pre-clinical AD individuals with or without cortical amyloid plaques [86–89], and in a recent fMRI study on the INSIGHT-preAD cohort [90]. From a neuro-cognitive point of view, mid-frontal cortices increase of theta rhythmogenesis in response to high amyloid deposition may either suggest a "compensatory brain mechanisms" (i.e., cognitive reserve) [4, 5, 91] to cope with amyloidosis, or a functional alteration of the DMN. In view of the absence of correlation between mid-frontal theta power and the individuals' cognitive scores (above all, memory), we tend to suggest that if any compensatory mechanism exists, this may not manifest at a cognitive level, but rather at a mere functional one. It may however be noted that our data might not sufficiently inform this debate and the absence of correlation between cognition and physiology could be expected in the present study, because 1) the INSIGHT-preAD individuals have been specifically selected for being cognitively intact from an objective point of view, and 2) importantly, no statistical difference exists at a behavioral level across the individuals of the INSIGHT-preAD cohort.

Surprisingly we did not find any effect of the APOE genotype on the mid-frontal theta dynamics while theta dynamics was correlated to amyloid load and amyloid load is known to be correlated with the APOE genotype [92, 93], and pre-symptomatic carriers of the APOE $\varepsilon 4$ allele with a higher amyloid load show a more rapid cognitive decline as compared to APOE $\varepsilon 4$ non-carriers [94]. However, to the best of our knowledge, only a few structural [95] or functional [16] neuroimaging studies, as well as a limited number of EEG investigations [96, 97] have fed in this hypothesis. In the present work, we can only provide evidence on the predominance of brain amyloidosis over APOE on the sources of brain rhythms and suggest further ad-hoc investigation to carefully disentangle the amyloid-APOE interaction. In this respect, future studies should consider not only determinist model of AD (as the amyloid cascade hypothesis), but also recent probabilistic models of AD [56] according to which three variants of AD (autosomal dominant AD, APOE $\varepsilon 4$-related sporadic AD, and APOE $\varepsilon 4$-unrelated sporadic AD) feature decreasing penetrance and decreasing weight of the amyloid pathophysiological cascade and increasing weight of stochastic factors (environmental exposures and lower-risk genes). Alternatively, APOE genotype-independent changes in EEG could be related to tau pathology which has not been assessed in the INSIGHT cohort yet. Future

EEG studies should also benefit from the combination of neuroimaging techniques and multimodal biomarker data, for example with novel functional neuroimaging genetics which should bring new evidence in the field [98].

Crucially, longitudinal source-level analyses provide insightful results to help inform the previous debate of any compensatory mechanisms to cope with cortical amyloidosis, and any implication of the DMN. In fact, while we did not replicate the difference at M24 in mid-frontal theta power between A+ and A−, analyses at M24 show that cortical amyloid status discriminated theta band power differences in the pre-cuneus/posterior-cingulate cortex. Neuroscience studies shows a major implication of this area on the AD spectrum. Particularly, while increased pre-cuneus atrophy has been associated to early-AD [99], higher amyloid load in this region characterizes a reduced cholinergic activity in overt AD [100, 101]. From a functional perspective, aberrant activity in this area [102], as well as a decreased connectivity between the pre-cuneus and the anterior DMN differentiates normal aging from AD [103] and can even target memory performances in prodromal AD [104]. Our results are not only in line with these findings, but also highlight for the first time a direct association of cortical amyloid load with the theta-band hyper-activation of the pre-cuneus in individuals at-risk for AD. Importantly, given the pivotal role that the pre-cuneus plays in the DMN [105] and the inverse relation between theta increase and DMN activation [85], such an increase of posterior theta oscillations can corroborate the hypothesis of an amyloid-driven hypo-activation of this network. Remarkably, here we provide the first evidence that theta oscillations behave like a non-static neurodynamic in the AD continuum [105–107] and that amyloid status modulates theta changes over two pivotal hubs of the DMN, namely the mid-frontal cortex and the pre-cuneus.

It is worth mentioning the absence of any significant difference in the alpha band, a frequency that has been convincingly associated to AD progression. From a qualitative viewpoint, here we only report a trend to a decrease of alpha band power as a function of the amyloid status at the second-year follow-up, thus suggesting that posterior alpha slowing, which is canonically associated to physiological aging, MCI, and AD, may emerge at later stages of the pre-AD. Alternatively, it might be hypothesized that in pre-AD the amyloid-driven alpha power changes also occur on different brain networks. While in this work we did not confirm this result, in a recent EEG study from the INSIGHT cohort (data not shown) we noticed an increase of alpha band activity in the frontal scalp-electrodes associated with an increased amyloid uptake, which raises a plateau at the threshold of amyloid positivity and then diminishes as amyloid burden increases.

On a final note, it is important to underline that this study is not associated to the prediction of the subjects' conversion to AD. Only 15 subjects from the INSIGHT-preAD study follow-up converted to prodromal AD by M60, namely 60 months after the first baseline visit (i.e., M0). Among those converters, only 4 individuals converted to prodromal AD by M24 (1 participant at M18 and 3 participants at M24). As soon as they were diagnosed, the participants were removed for the INSIGHT-preAD study (and followed in another cohort). The fact that after 2 years follow-up, only 4 participants converted to prodromal AD prevented us from running statistical analysis that may lead to meaningful clinical and neurological interpretation, especially in reference to any correlation between EEG changes, amyloid burden, and APOE pattern. Other relevant questions that should be addressed concern the type of dementia that converters might develop, and whether such conversion is driven by the initial burden of amyloidosis. Future follow-up studies on the INSIGHT-preAD cohort will allow further tracking of the evolution of the EEG dynamics as a function or as predictors of individuals' conversion to clinical stages of AD, namely prodromal (predementia) and dementia stages.

Conclusions

In conclusion, we provide the first longitudinal evidence on the impact of brain amyloidosis on the EEG dynamics of a large-scale, monocentric cohort of elderly subjective memory complainers at-risk for AD in terms of pathophysiological biomarker burden (that is, amyloidosis). We show that different neural markers are in play at different time points of the follow-up. Theta band power increase seems associated with amyloidosis. Moreover, theta power highlights a potential travelling property, such that its plastic transition from the anterior to the posterior DMN characterized the two stages of the follow-up. Noteworthy, alpha band power slowing showed a decremental tendency at the second-year follow-up, albeit with a relatively poor statistical power. Future follow-up studies on the INSIGHT-preAD cohort will allow further tracking of the evolution of such EEG

dynamics, in particular in relation to the conversion to prodromal AD, which was beyond the scope of this study.

ACKNOWLEDGMENTS

REFERENCES

[1] Braak H, Braak E (1991) Neuropathological stageing of Alzheimer-related changes. *Acta Neuropathol* **82**, 239-259.

[2] Duyckaerts C, Delatour B, Potier M-C (2009) Classification and basic pathology of Alzheimer disease. *Acta Neuropathol* **118**, 5-36.

[3] Cummings JL, Morstorf T, Zhong K (2014) Alzheimer's disease drug-development pipeline: Few candidates, frequent failures. *Alzheimers Res Ther* **6**, 37.

[4] STERN Y (2002) What is cognitive reserve? Theory and research application of the reserve concept. *J Int Neuropsychol Soc* **8**, 448-460.

[5] Stern Y (2012) Cognitive reserve in ageing and Alzheimer's disease. *Lancet Neurol* **11**, 1006-1012.

[6] Olazarán J, Muñiz R, Reisberg B, Peña-Casanova J, del Ser T, Cruz-Jentoft AJ, Serrano P, Navarro E, García de la Rocha ML, Frank A, Galiano M, Fernández-Bullido Y, Serra JA, González-Salvador MT, Sevilla C (2004) Benefits of cognitive-motor intervention in MCI and mild to moderate Alzheimer disease. *Neurology* **63**, 2348-2353.

[7] Solé-Padullés C, Bartrés-Faz D, Junqué C, Vendrell P, Rami L, Clemente IC, Bosch B, Villar A, Bargalló N, Jurado MA, Barrios M, Molinuevo JL (2009) Brain structure and function related to cognitive reserve variables in normal aging, mild cognitive impairment and Alzheimer's disease. *Neurobiol Aging* **30**, 1114-1124.

[8] Amodio P, Montagnese S, Spinelli G, Schiff S, Mapelli D (2017) Cognitive reserve is a resilience factor for cognitive dysfunction in hepatic encephalopathy. *Metab Brain Dis* **32**, 1287-1293.

[9] Hardy JA, Higgins GA (1992) Alzheimer's disease: The amyloid cascade hypothesis. *Science* **256**, 184-185.

[10] Selkoe DJ, Hardy J (2016) The amyloid hypothesis of Alzheimer's disease at 25 years. *EMBO Mol Med* **8**, 595-608.

[11] Walsh C, Drinkenburg WHIM, Ahnaou A (2017) Neurophysiological assessment of neural network plasticity and connectivity: Progress towards early functional biomarkers for disease interception therapies in Alzheimer's disease. *Neurosci Biobehav Rev* **73**, 340-358.

[12] Jack CR, Knopman DS, Jagust WJ, Petersen RC, Weiner MW, Aisen PS, Shaw LM, Vemuri P, Wiste HJ, Weigand SD, Lesnick TG, Pankratz VS, Donohue MC, Trojanowski JQ (2013) Tracking pathophysiological processes in Alzheimer's disease: An updated hypothetical model of dynamic biomarkers. *Lancet Neurol* **12**, 207-216.

[13] Brier MR, Thomas JB, Ances BM (2014) Network dysfunction in Alzheimer's disease: Refining the disconnection hypothesis. *Brain Connect* **4**, 299-311.

[14] Williams MM, Xiong C, Morris JC, Galvin JE (2006) Survival and mortality differences between dementia with Lewy bodies vs Alzheimer disease. *Neurology* **67**, 1935-1941.

[15] Hampel H, Toschi N, Babiloni C, Baldacci F, Black KL, Bokde ALW, Bun RS, Cacciola F, Cavedo E, Chiesa PA, Colliot O, Coman C-M, Dubois B, Duggento A, Durrleman S, Ferretti M-T, George N, Genthon R, Habert M-O, Herholz K, Koronyo Y, Koronyo-Hamaoui M, Lamari F, Langevin T, Lehéricy S, Lorenceau J, Neri C, Nisticò R, Nyasse-Messene F, Ritchie C, Rossi S, Santarnecchi E, Sporns O, Verdooner SR, Vergallo A, Villain N, Younesi E, Garaci F, Lista S (2018) Revolution of Alzheimer Precision neurology. Passageway of systems biology and neurophysiology. *J Alzheimers Dis* **64**, S47-S105.

[16] Chiesa PA, Cavedo E, Grothe MJ, Teipel SJ, Hampel H (2019) Basal forebrain resting functional activity associated with brain amyloid-beta burden in epsilon 4 carriers and older women: Possible implications for baseline cognition and response to amyloid-beta-based preventive trials response. *Radiology* **290**, 851.

[17] Dumitrescu L, Barnes LL, Thambisetty M, Beecham G, Kunkle B, Bush WS, Gifford KA, Chibnik LB, Mukherjee S, De Jager PL, Kukull W, Crane PK, Resnick SM, Keene CD, Montine TJ, Schellenberg GD, Deming Y, Chao MJ, Huentelman M, Martin ER, Hamilton-Nelson K, Shaw LM, Trojanowski JQ, Peskind ER, Cruchaga C, Pericak-Vance MA, Goate AM, Cox NJ, Haines JL, Zetterberg H, Blennow K, Larson EB, Johnson SC, Albert M, Initiative ADGC and the ADN, Bennett DA, Schneider JA, Jefferson AL, Hohman TJ (2019) Sex differences in the genetic predictors of Alzheimer's pathology. *Brain* **142**, 2581-2589.

[18] Cavedo E, Chiesa PA, Houot M, Ferretti MT, Grothe MJ, Teipel SJ, Lista S, Habert M-O, Potier M-C, Dubois B, Hampel H, Bakardjian H, Benali H, Bertin H, Bonheur J,

Boukadida L, Boukerrou N, Cavedo E, Chiesa P, Colliot O, Dubois B, Dubois M, Epelbaum S, Gagliardi G, Genthon R, Habert M-O, Hampel H, Houot M, Kas A, Lamari F, Levy M, Lista S, Metzinger C, Mochel F, Nyasse F, Poisson C, Potier M-C, Revillon M, Santos A, Andrade KS, Sole M, Surtee M, de Schotten MT, Vergallo A, Younsi N, Aguilar LF, Babiloni C, Baldacci F, Benda N, Black KL, Bokde ALW, Bonuccelli U, Broich K, Bun RS, Cacciola F, Castrillo J, Cavedo E, Ceravolo R, Chiesa PA, Colliot O, Coman C-M, Corvol J-C, Cuello AC, Cummings JL, Depypere H, Dubois B, Duggento A, Durrleman S, Escott-Price V, Federoff H, Ferretti MT, Fiandaca M, Frank RA, Garaci F, Genthon R, George N, Giorgi FS, Graziani M, Haberkamp M, Habert M-O, Hampel H, Herholz K, Karran E, Kim SH, Koronyo Y, Koronyo-Hamaoui M, Lamari F, Langevin T, Lehéricy S, Lista S, Lorenceau J, Mapstone M, Neri C, Nisticò R, Nyasse-Messene F, O'bryant SE, Perry G, Ritchie C, Rojkova K, Rossi S, Saidi A, Santarnecchi E, Schneider LS, Sporns O, Toschi N, Verdooner SR, Vergallo A, Villain N, Welikovitch LA, Woodcock J, Younesi E (2018) Sex differences in functional and molecular neuroimaging biomarkers of Alzheimer's disease in cognitively normal older adults with subjective memory complaints. *Alzheimers Dement* **14**, 1204-1215.

[19] Ferretti MT, Iulita MF, Cavedo E, Chiesa PA, Schumacher Dimech A, Santuccione Chadha A, Baracchi F, Girouard H, Misoch S, Giacobini E, Depypere H, Hampel H (2018) Sex differences in Alzheimer disease — the gateway to precision medicine. *Nat Rev Neurol* **14**, 457-469.

[20] Dubois B, Hampel H, Feldman HH, Scheltens P, Aisen P, Andrieu S, Bakardjian H, Benali H, Bertram L, Blennow K, Broich K, Cavedo E, Crutch S, Dartigues J-F, Duyckaerts C, Epelbaum S, Frisoni GB, Gauthier S, Genthon R, Gouw AA, Habert M-O, Holtzman DM, Kivipelto M, Lista S, Molinuevo J-L, O'Bryant SE, Rabinovici GD, Rowe C, Salloway S, Schneider LS, Sperling R, Teichmann M, Carrillo MC, Cummings J, Jack CR (2016) Preclinical Alzheimer's disease: Definition, natural history, and diagnostic criteria. *Alzheimers Dement* **12**, 292-323.

[21] Klimesch W (1999) EEG alpha and theta oscillations reflect cognitive and memory performance: A review and analysis. *Brain Res Rev* **29**, 169-195.

[22] Babiloni C, Binetti G, Cassarino A, Dal Forno G, Del Percio C, Ferreri F, Ferri R, Frisoni G, Galderisi S, Hirata K, Lanuzza B, Miniussi C, Mucci A, Nobili F, Rodriguez G, Luca Romani G, Rossini PM (2006) Sources of cortical rhythms in adults during physiological aging: A multicentric EEG study. *Hum Brain Mapp* **27**, 162-172.

[23] Babiloni C, Binetti G, Cassetta E, Forno GD, Percio C Del, Ferreri F, Ferri R, Frisoni G, Hirata K, Lanuzza B, Miniussi C, Moretti D V, Nobili F, Rodriguez G, Romani GL, Salinari S, Rossini PM (2006) Sources of cortical rhythms change as a function of cognitive impairment in pathological aging: A multicenter study. *Clin Neurophysiol* **117**, 252-268.

[24] Babiloni C, Frisoni G, Steriade M, Bresciani L, Binetti G, Delpercio C, Geroldi C, Miniussi C, Nobili F, Rodriguez G (2006) Frontal white matter volume and delta EEG sources negatively correlate in awake subjects with mild cognitive impairment and Alzheimer's disease. *Clin Neurophysiol* **117**, 1113-1129.

[25] Babiloni C, Vecchio F, Lizio R, Ferri R, Rodriguez G, Marzano N, Frisoni GB, Rossini PM (2011) Resting state cortical rhythms in mild cognitive impairment and

Alzheimer's disease: Electroencephalographic evidence. *J Alzheimers Dis* **26**, 201-214.

[26] Klimesch W (2012) α-band oscillations, attention, and controlled access to stored information. *Trends Cogn Sci* **16**, 606-617.

[27] Rossini PM, Del Percio C, Pasqualetti P, Cassetta E, Binetti G, Dal Forno G, Ferreri F, Frisoni G, Chiovenda P, Miniussi C, Parisi L, Tombini M, Vecchio F, Babiloni C (2006) Conversion from mild cognitive impairment to Alzheimer's disease is predicted by sources and coherence of brain electroencephalography rhythms. *Neuroscience* **143**, 793-803.

[28] Misra C, Fan Y, Davatzikos C (2009) Baseline and longitudinal patterns of brain atrophy in MCI patients, and their use in prediction of short-term conversion to AD: Results from ADNI. *Neuroimage* **44**, 1415-1422.

[29] Penttilä M, Partanen JV, Soininen H, Riekkinen PJ (1985) Quantitative analysis of occipital EEG in different stages of Alzheimer's disease. *Electroencephalogr Clin Neurophysiol* **60**, 1-6.

[30] Huang C, Wahlund L-O, Dierks T, Julin P, Winblad B, Jelic V (2000) Discrimination of Alzheimer's disease and mild cognitive impairment by equivalent EEG sources: A cross-sectional and longitudinal study. *Clin Neurophysiol* **111**, 1961-1967.

[31] Moretti D (2004) Individual analysis of EEG frequency and band power in mild Alzheimer's disease. *Clin Neurophysiol* **115**, 299-308.

[32] Musaeus CS, Engedal K, Høgh P, Jelic V, Mørup M, Naik M, Oeksengaard A-R, Snaedal J, Wahlund L-O, Waldemar G, Andersen BB (2018) EEG theta power is an early marker of cognitive decline in dementia due to Alzheimer's disease. *J Alzheimers Dis* **64**, 1359-1371.

[33] Tombaugh TN, McIntyre NJ (1992) The Mini-Mental State Examination: A comprehensive review. *J Am Geriatr Soc* **40**, 922-935.

[34] Del Percio C, Bevilacqua V, Brunetti A, Lizio R, Soricelli A, Ferri R, Nobili F, Gesualdo L, Logroscino G, De Tommaso M, Triggiani AI, Blūma M, Frisoni GB, Babiloni C (2019) Classification of healthy subjects and Alzheimer's disease patients with dementia from cortical sources of resting state EEG rhythms: Comparing different approaches. In *Converging Clinical and Engineering Research on Neurorehabilitation III. ICNR 2018. Biosystems & Biorobotics,* vol 21, Masia L, Micera S, Akay M, Pons J, eds. Springer, Cham, pp. 977-981.

[35] Durongbhan P, Zhao Y, Chen L, Zis P, De Marco M, Unwin ZC, Venneri A, He X, Li S, Zhao Y, Blackburn DJ, Sarrigiannis PG (2019) A dementia classification framework using frequency and time-frequency features based on EEG signals. *IEEE Trans Neural Syst Rehabil Eng* **27**, 826-835.

[36] Gallego-Jutglà E, Solé-Casals J, Vialatte F-B, Dauwels J, Cichocki A (2014) A theta-band EEG based index for early diagnosis of Alzheimer's disease. *J Alzheimers Dis* **43**, 1175-1184.

[37] Al-Qazzaz NK, Ali SHBM, Ahmad SA, Islam MS, Escudero J (2017) Discrimination of stroke-related mild cognitive impairment and vascular dementia using EEG signal analysis. *Med Biol Eng Comput* **56**, 137-157.

[38] Goodman MS, Kumar S, Zomorrodi R, Ghazala Z, Cheam ASM, Barr MS, Daskalakis ZJ, Blumberger DM, Fischer C, Flint A, Mah L, Herrmann N, Bowie CR, Mulsant BH, Rajji TK (2018) Theta-gamma coupling and work-

ing memory in Alzheimer's dementia and mild cognitive impairment. *Front Aging Neurosci* **10**, 101.

[39] Peraza LR, Cromarty R, Kobeleva X, Firbank MJ, Killen A, Graziadio S, Thomas AJ, O'Brien JT, Taylor J-P (2018) Electroencephalographic derived network differences in Lewy body dementia compared to Alzheimer's disease patients. *Sci Rep* **8**, 4637.

[40] Cuesta P, Garcés P, Castellanos NP, López ME, Aurtenetxe S, Bajo R, Pineda-Pardo JA, Bruña R, Marín AG, Delgado M, Barabash A, Ancín I, Cabranes JA, Fernandez A, Del Pozo F, Sancho M, Marcos A, Nakamura A, Maestú F (2015) Influence of the APOE ε4 allele and mild cognitive impairment diagnosis in the disruption of the MEG resting state functional connectivity in sources space. *J Alzheimers Dis* **44**, 493-505.

[41] Lehtovirta M, Partanen J, Könönen M, Soininen H, Helisalmi S, Mannermaa A, Ryynänen M, Hartikainen P, Riekkinen P (1996) Spectral analysis of EEG in Alzheimer's disease: Relation to apolipoprotein E polymorphism. *Neurobiol Aging* **17**, 523-526.

[42] Gonzalez-Escamilla G, Atienza M, Cantero JL (2014) Impaired cortical oscillatory coupling in mild cognitive impairment: Anatomical substrate and ApoE4 effects. *Brain Struct Funct* **220**, 1721-1737.

[43] Michels L, Muthuraman M, Anwar AR, Kollias S, Leh SE, Riese F, Unschuld PG, Siniatchkin M, Gietl AF, Hock C (2017) Changes of functional and directed resting-state connectivity are associated with neuronal oscillations, ApoE genotype and amyloid deposition in mild cognitive impairment. *Front Aging Neurosci* **9**, 304.

[44] Koelewijn L, Lancaster TM, Linden D, Dima DC, Routley BC, Magazzini L, Barawi K, Brindley L, Adams R, Tansey KE, Bompas A, Tales A, Bayer A, Singh K (2019) Oscillatory hyperactivity and hyperconnectivity in young APOE-ε4 carriers and hypoconnectivity in Alzheimer's disease. *Elife* **8**, e36011.

[45] Brunovsky M, Matousek M, Edman A, Cervena K, Krajca V (2003) Objective assessment of the degree of dementia by means of EEG. *Neuropsychobiology* **48**, 19-26.

[46] Stam CJ, Montez T, Jones BF, Rombouts SARB, van der Made Y, Pijnenburg YAL, Scheltens P (2005) Disturbed fluctuations of resting state EEG synchronization in Alzheimer's disease. *Clin Neurophysiol* **116**, 708-715.

[47] Vecchio F, Miraglia F, Iberite F, Lacidogna G, Guglielmi V, Marra C, Pasqualetti P, Tiziano FD, Rossini PM (2018) Sustainable method for Alzheimer dementia prediction in mild cognitive impairment: Electroencephalographic connectivity and graph theory combined with apolipoprotein E. *Ann Neurol* **84**, 302-314.

[48] Stam CJ, Jones BF, Nolte G, Breakspear M, Scheltens P (2007) Small-world networks and functional connectivity in Alzheimer's disease. *Cereb Cortex* **17**, 92-9.

[49] Babiloni C, Frisoni G, Vecchio F, Lizio R, Pievani M, Geroldi C, Fracassi C, Vernieri F, Ursini F, Rodriguez G, Nobili F, Salinari S, Van Dijkman S, Ferri R, Rossini PM (2009) Global functional coupling of resting EEG rhythms is abnormal in mild cognitive impairment and Alzheimer's disease. *J Psychophysiol* **23**, 224-234.

[50] Li Y, Wang X, Li Y, Sun Y, Sheng C, Li H, Li X, Yu Y, Chen G, Hu X, Jing B, Wang D, Li K, Jessen F, Xia M, Han Y, Li Y, Wang X, Li Y, Sun Y, Sheng C, Li H, Li X, Yu Y, Chen G, Hu X, Jing B, Wang D, Li K, Jessen F, Xia M, Han Y (2016) Abnormal resting-state functional connectivity strength in mild cognitive impairment and its conversion to Alzheimer's disease. *Neural Plast* **2016**, 4680972.

[51] Yu M, Gouw AA, Hillebrand A, Tijms BM, Stam CJ, van Straaten ECW, Pijnenburg YAL (2016) Different functional connectivity and network topology in behavioral variant of frontotemporal dementia and Alzheimer's disease: An EEG study. *Neurobiol Aging* **42**, 150-162.

[52] de Haan W, van Straaten ECW, Gouw AA, Stam CJ (2017) Altering neuronal excitability to preserve network connectivity in a computational model of Alzheimer's disease. *PLoS Comput Biol* **13**, e1005707.

[53] Guillon J, Attal Y, Colliot O, La Corte V, Dubois B, Schwartz D, Chavez M, De Vico Fallani F (2017) Loss of brain inter-frequency hubs in Alzheimer's disease. *Sci Rep* **7**, 10879.

[54] Babiloni C, Del Percio C, Lizio R, Noce G, Lopez S, Soricelli A, Ferri R, Nobili F, Arnaldi D, Famà F, Aarsland D, Orzi F, Buttinelli C, Giubilei F, Onofrj M, Stocchi F, Stirpe P, Fuhr P, Gschwandtner U, Ransmayr G, Garn H, Fraioli L, Pievani M, Frisoni GB, D'Antonio F, De Lena C, Güntekin B, Hanoğlu L, Başar E, Yener G, Emek-Savaş DD, Triggiani AI, Franciotti R, Taylor JP, Vacca L, De Pandis MF, Bonanni L (2018) Abnormalities of resting-state functional cortical connectivity in patients with dementia due to Alzheimer's and Lewy body diseases: An EEG study. *Neurobiol Aging* **65**, 18-40.

[55] Vecchio F, Babiloni C, Lizio R, De Vico Fallani F, Blinowska K, Verrienti G, Frisoni G, Rossini PM (2013) Resting state cortical EEG rhythms in Alzheimer's disease. *Appl Brain Oscil Neuropsychiatr Dis - Sel Pap from "Brain Oscil Cogn Impair Neurotransmitters" Conf Istanbul, Turkey, 29 April May 2011*, pp. 223-236.

[56] Frisoni GB, Altomare D, Thal DR, Ribaldi F, van der Kant R, Ossenkoppele R, Blennow K, Cummings J, van Duijn C, Nilsson PM, Dietrich P-Y, Scheltens P, Dubois B (2022) The probabilistic model of Alzheimer disease: The amyloid hypothesis revised. *Nat Rev Neurosci* **23**, 53-66.

[57] Jonker C, Geerlings MI, Schmand B (2000) Are memory complaints predictive for dementia? A review of clinical and population-based studies. *Int J Geriatr Psychiatry* **15**, 983-991.

[58] Babiloni C, Visser PJ, Frisoni G, De Deyn PP, Bresciani L, Jelic V, Nagels G, Rodriguez G, Rossini PM, Vecchio F, Colombo D, Verhey F, Wahlund L-O, Nobili F (2010) Cortical sources of resting EEG rhythms in mild cognitive impairment and subjective memory complaint. *Neurobiol Aging* **31**, 1787-1798.

[59] Prichep LS, John ER, Ferris SH, Rausch L, Fang Z, Cancro R, Torossian C, Reisberg B (2006) Prediction of longitudinal cognitive decline in normal elderly with subjective complaints using electrophysiological imaging. *Neurobiol Aging* **27**, 471-481.

[60] Gouw AA, Alsema AM, Tijms BM, Borta A, Scheltens P, Stam CJ, van der Flier WM (2017) EEG spectral analysis as a putative early prognostic biomarker in nondemented, amyloid positive subjects. *Neurobiol Aging* **57**, 133-142.

[61] Dubois B, Epelbaum S, Nyasse F, Bakardjian H, Gagliardi G, Uspenskaya O, Houot M, Lista S, Cacciamani F, Potier M-C, Bertrand A, Lamari F, Benali H, Mangin J-F, Colliot O, Genthon R, Habert M-O, Hampel H, Audrain C, Auffret A, Baldacci F, Benakki I, Bertin H, Boukadida L, Cavedo E, Chiesa P, Dauphinot L, Dos Santos A, Dubois M, Durrleman S, Fontaine G, Genin A, Glasman P, Jungalee N, Kas A, Kilani M, La Corte V, Lehericy S, Letondor C, Levy M, Lowrey M, Ly J, Makiese O, Metzinger C, Michon A, Mochel F, Poisson C, Ratovohery S, Revillon M, Rojkova K, Roy P, Santos-Andrade K, Schindler R,

Seux L, Simon V, Sole M, Tandetnik C, Teichmann M, Thiebaut de Shotten M, Younsi N (2018) Cognitive and neuroimaging features and brain β-amyloidosis in individuals at risk of Alzheimer's disease (INSIGHT-preAD): A longitudinal observational study. *Lancet Neurol* **17**, 335-346.

[62] Teipel S, Bakardjian H, Gonzalez-Escamilla G, Cavedo E, Weschke S, Dyrba M, Grothe MJ, Potier M-C, Habert M-O, Dubois B, Hampel H, INSIGHT-preAD study group (2017) No association of cortical amyloid load and EEG connectivity in older people with subjective memory complaints. *Neuroimage Clin* **17**, 435-443.

[63] Gaubert S, Raimondo F, Houot M, Corsi MC, Naccache L, Sitt JD, Hermann B, Oudiette D, Gagliardi G, Habert MO, Dubois B, De Vico Fallani F, Bakardjian H, Epelbaum S (2019) EEG evidence of compensatory mechanisms in preclinical Alzheimer's disease. *Brain* **142**, 2096-2112.

[64] Morris JC (1993) The Clinical Dementia Rating (CDR). *Neurology* **43**, 2412.2-2412-a.

[65] Wechsler D (1945) A standardized memory scale for clinical use. *J Psychol* **19**, 87-95.

[66] Fastenau PS, Denburg NL, Hufford BJ (1999) Adult norms for the Rey-Osterrieth Complex Figure Test and for supplemental recognition and matching trials from the Extended Complex Figure Test. *Clin Neuropsychol* **13**, 30-47.

[67] Tombaugh TN (2004) Trail Making Test A and B: Normative data stratified by age and education. *Arch Clin Neuropsychol* **19**, 203-214.

[68] Dubois B, Slachevsky A, Litvan I, Pillon B (2000) The FAB: A frontal assessment battery at bedside. *Neurology* **55**, 1621-1626.

[69] Rentz DM, Parra Rodriguez MA, Amariglio R, Stern Y, Sperling R, Ferris S (2013) Promising developments in neuropsychological approaches for the detection of preclinical Alzheimer's disease: A selective review. *Alzheimers Res Ther* **5**, 58.

[70] McLeod DR, Griffiths RR, Bigelow GE, Yingling J (1982) An automated version of the digit symbol substitution test (DSST). *Behav Res Methods Instrum* **14**, 463-466.

[71] Besson FL, La Joie R, Doeuvre L, Gaubert M, Mezenge F, Egret S, Landeau B, Barre L, Abbas A, Ibazizene M, de La Sayette V, Desgranges B, Eustache F, Chetelat G (2015) Cognitive and brain profiles associated with current neuroimaging biomarkers of preclinical Alzheimer's disease. *J Neurosci* **35**, 10402-10411.

[72] Habert M-O, Bertin H, Labit M, Diallo M, Marie S, Martineau K, Kas A, Causse-Lemercier V, Bakardjian H, Epelbaum S, Chételat G, Houot M, Hampel H, Dubois B, Mangin J-F (2018) Evaluation of amyloid status in a cohort of elderly individuals with memory complaints: Validation of the method of quantification and determination of positivity thresholds. *Ann Nucl Med* **32**, 75-86.

[73] Oostenveld R, Fries P, Maris E, Schoffelen J-M (2011) FieldTrip: Open source software for advanced analysis of MEG, EEG, and invasive electrophysiological data. *Comput Intell Neurosci* **2011**, 156869.

[74] Oostendorp TF, van Oosterom A (1989) Source parameter estimation in inhomogeneous volume conductors of arbitrary shape. *IEEE Trans Biomed Eng* **36**, 382-391.

[75] Van Veen BD, Van Drongelen W, Yuchtman M, Suzuki A (1997) Localization of brain electrical activity via linearly constrained minimum variance spatial filtering. *IEEE Trans Biomed Eng* **44**, 867-880.

[76] Tzourio-Mazoyer N, Landeau B, Papathanassiou D, Crivello F, Etard O, Delcroix N, Mazoyer B, Joliot M (2002) Automated anatomical labeling of activations in SPM using a macroscopic anatomical parcellation of the MNI MRI single-subject brain. *Neuroimage* **15**, 273-289.

[77] Maris E, Oostenveld R (2007) Nonparametric statistical testing of EEG- and MEG-data. *J Neurosci Methods* **164**, 177-190.

[78] Mewhort DJK, Kelly M, Johns BT (2009) Randomization tests and the unequal-N/unequal-variance problem. *Behav Res Methods* **41**, 664-667.

[79] Siapas AG, Lubenov EV, Wilson MA (2005) Prefrontal phase locking to hippocampal theta oscillations. *Neuron* **46**, 141-151.

[80] Mitchell DJ, McNaughton N, Flanagan D, Kirk IJ (2008) Frontal-midline theta from the perspective of hippocampal "theta." *Prog Neurobiol* **86**, 156-185.

[81] Jones MW, Wilson MA (2005) Theta rhythms coordinate hippocampal-prefrontal interactions in a spatial memory task. *PLoS Biol* **3**, e402-e402.

[82] Buzsáki G, Moser EI (2013) Memory, navigation and theta rhythm in the hippocampal-entorhinal system. *Nat Neurosci* **16**, 130-138.

[83] Tambini A, Nee DE, D'Esposito M (2018) Hippocampal-targeted theta-burst stimulation enhances associative memory formation. *J Cogn Neurosci* **30**, 1452-1472.

[84] Backus AR, Schoffelen J-M, Szebényi S, Hanslmayr S, Doeller CF (2016) Hippocampal-prefrontal theta oscillations support memory integration. *Curr Biol* **26**, 450-457.

[85] Scheeringa R, Bastiaansen MCM, Petersson KM, Oostenveld R, Norris DG, Hagoort P (2008) Frontal theta EEG activity correlates negatively with the default mode network in resting state. *Int J Psychophysiol* **67**, 242-251.

[86] Greicius MD, Srivastava G, Reiss AL, Menon V (2004) Default-mode network activity distinguishes Alzheimer's disease from healthy aging: Evidence from functional MRI. *Proc Natl Acad Sci U S A* **101**, 4637-42.

[87] Greicius MD, Supekar K, Menon V, Dougherty RF (2009) Resting-state functional connectivity reflects structural connectivity in the default mode network. *Cereb Cortex* **19**, 72-78.

[88] Sheline YI, Raichle ME, Snyder AZ, Morris JC, Head D, Wang S, Mintun MA (2010) Amyloid plaques disrupt resting state default mode network connectivity in cognitively normal elderly. *Biol Psychiatry* **67**, 584-587.

[89] Jones DT, Machulda MM, Vemuri P, McDade EM, Zeng G, Senjem ML, Gunter JL, Przybelski SA, Avula RT, Knopman DS, Boeve BF, Petersen RC, Jack CR (2011) Age-related changes in the default mode network are more advanced in Alzheimer disease. *Neurology* **77**, 1524-1531.

[90] Chiesa PA, Cavedo E, Vergallo A, Lista S, Potier M-C, Habert M-O, Dubois B, de Schotten MT, Hampel H, Bakardjian H (2019) Differential default mode network trajectories in asymptomatic individuals at risk for Alzheimer's disease. *Alzheimers Dement* **15**, 940-950.

[91] Stern Y (2006) Cognitive reserve and Alzheimer disease. *Alzheimer Dis Assoc Disord* **20**, S69-S74.

[92] Morris JC, Roe CM, Xiong C, Fagan AM, Goate AM, Holtzman DM, Mintun MA (2010) APOE predicts amyloid-beta but not tau Alzheimer pathology in cognitively normal aging. *Ann Neurol* **67**, 122-131.

[93] Dubois B, Hampel H, Feldman HH, Scheltens P, Aisen P, Andrieu S, Bakardjian H, Benali H, Bertram L, Blennow K, Broich K, Cavedo E, Crutch S, Dartigues J-F, Duyckaerts C, Epelbaum S, Frisoni GB, Gauthier S, Genthon R,

Gouw AA, Habert M-O, Holtzman DM, Kivipelto M, Lista S, Molinuevo J-L, O'Bryant SE, Rabinovici GD, Rowe C, Salloway S, Schneider LS, Sperling R, Teichmann M, Carrillo MC, Cummings J, Jack Jr CR, Proceedings of the Meeting of the International Working Group (IWG) and the American Alzheimer's Association on "The Preclinical State of AD"; July 23 USA 2015; Washington DC (2016) Preclinical Alzheimer's disease: Definition, natural history, and diagnostic criteria. *Alzheimers Dement* **12**, 292-323.

[94] Mormino EC, Betensky RA, Hedden T, Schultz AP, Ward A, Huijbers W, Rentz DM, Johnson KA, Sperling RA (2014) Amyloid and APOE 4 interact to influence short-term decline in preclinical Alzheimer disease. *Neurology* **82**, 1760-1767.

[95] Dowell NG, Evans SL, Tofts PS, King SL, Tabet N, Rusted JM (2016) Structural and resting-state MRI detects regional brain differences in young and mid-age healthy APOE-e4 carriers compared with non-APOE-e4 carriers. *NMR Biomed* **29**, 614-624.

[96] Canuet L, Tellado I, Couceiro V, Fraile C, Fernandez-Novoa L, Ishii R, Takeda M, Cacabelos R (2012) Resting-state network disruption and APOE genotype in Alzheimer's disease: A lagged functional connectivity study. *PLoS One* **7**, e46289.

[97] Hatz F, Benz N, Hardmeier M, Zimmermann R, Rueegg S, Schindler C, Miserez AR, Gschwandtner U, Monsch AU, Fuhr P (2013) Quantitative EEG and apolipoprotein E genotype improve classification of patients with suspected Alzheimer's disease. *Clin Neurophysiol* **124**, 2146-2152.

[98] Chiesa PA, Cavedo E, Lista S, Thompson PM, Hampel H (2017) Revolution of resting-state functional neuroimaging genetics in Alzheimer's disease. *Trends Neurosci* **40**, 469-480.

[99] Karas G, Scheltens P, Rombouts S, van Schijndel R, Klein M, Jones B, van der Flier W, Vrenken H, Barkhof F (2007) Precuneus atrophy in early-onset Alzheimer's disease: A morphometric structural MRI study. *Neuroradiology* **49**, 967-976.

[100] Ikonomovic MD, Klunk WE, Abrahamson EE, Wuu J, Mathis CA, Scheff SW, Mufson EJ, DeKosky ST (2011) Precuneus amyloid burden is associated with reduced cholinergic activity in Alzheimer disease. *Neurology* **77**, 39-47.

[101] Stricker NH, Dodge HH, Dowling NM, Han SD, Erosheva EA, Jagust WJ, Initiative ADN (2012) CSF biomarker associations with change in hippocampal volume and precuneus thickness: Implications for the Alzheimer's pathological cascade. *Brain Imaging Behav* **6**, 599-609.

[102] Rami L, Sala-Llonch R, Solé-Padullés C, Fortea J, Olives J, Lladó A, Peña-Gómez C, Balasa M, Bosch B, Antonell A, Sanchez-Valle R, Bartrés-Faz D, Molinuevo JL (2012) Distinct functional activity of the precuneus and posterior cingulate cortex during encoding in the preclinical stage of Alzheimer's disease. *J Alzheimers Dis* **31**, 517-526.

[103] Klaassens BL, van Gerven JMA, van der Grond J, de Vos F, Möller C, Rombouts SARB (2017) Diminished posterior precuneus connectivity with the default mode network differentiates normal aging from Alzheimer's disease. *Front Aging Neurosci* **9**, 97.

[104] Koch G, Bonnì S, Pellicciari MC, Casula EP, Mancini M, Esposito R, Ponzo V, Picazio S, Di Lorenzo F, Serra L, Motta C, Maiella M, Marra C, Cercignani M, Martorana A, Caltagirone C, Bozzali M (2018) Transcranial magnetic stimulation of the precuneus enhances memory and neural activity in prodromal Alzheimer's disease. *Neuroimage* **169**, 302-311.

[105] Fransson P, Marrelec G (2008) The precuneus/posterior cingulate cortex plays a pivotal role in the default mode network: Evidence from a partial correlation network analysis. *Neuroimage* **42**, 1178-1184.

[106] Lubenov EV, Siapas AG (2009) Hippocampal theta oscillations are travelling waves. *Nature* **459**, 534-539.

[107] Muller L, Chavane F, Reynolds J, Sejnowski TJ (2018) Cortical travelling waves: Mechanisms and computational principles. *Nat Rev Neurosci* **19**, 255-268.